Integral sliding-mode control of phase shift for two-rotor vibration setup

N. Kuznetsov[1,2], I. Boiko [3], B. Andrievsky[1,2], E. Kudryashova[1], O. Kuznetsova[1], and I. Zaitceva [1,2]

***Abstract*— This paper focuses on developing and studying a phase shift control system for a two-rotor vibration mechatronic setup. The controller serves to maintain the desired revolving speed of the unbalanced rotors and the desired phase shift between them. The sliding mode motion is achieved using an integral relay controller in the phase loop, while PI controllers are employed in the velocity control loops. The numerical study, simulations, and experiments are performed using the Mechatronic Vibration Setup SV-2M. The velocity and phase shift control laws are studied, and the possibility of asymptotic sliding mode occurrence in the phase shift loop is examined through analytical and numerical analysis. The simulation and experimental results confirm the asymptotic emergence of sliding mode motion and demonstrate the dynamical properties of the closed-loop system.**

***Index Terms*— Phase shift control; Two-rotor vibration mechatronic setup; Induction motor; Sliding mode motion; Relay control; PI control**

I. Introduction

Vibration technologies find application across diverse industries and manufacturing sectors, such as ore enrichment, metallurgy, mechanical engineering, chemical industries, production of construction materials, grinding, fine grinding, and surface treatment of various parts. A vibration machine is an assembly where the working element undergoes oscillatory motion essential for executing or enhancing a specific process. These machines can be categorized based on various factors such as the drive type, energy transformation, spectral composition of generated vibration, trajectory shape of the working element, and others. The phenomenon of vibration-induced rotation maintenance enhances motor efficiency, utilized in cone crushers. Machines in mineral processing, construction, chemical, and food industries operate on the principle of vibration displacement. The artificial mode of multiple synchronization is implemented by different (multiple) rotational frequencies of the rotors, forming complex shapes and heterogeneous trajectory fields of the points on the vibrator. This effect expands the technological possibilities of using vibration machines for performing challenging transportation tasks, such as the movement of dusty, wet, and sticky loads, as well as simultaneous screening and separation of bulk materials. Asymmetry of vibrations at multiple rotor speeds creates and enhances vibratory conveying with increased productivity.

The primary operational modes and control of a vibration system include start-up, passage through resonance, and synchronization. Specifically considering movement in the vertical plane while disregarding deviations from planar parallel motion, synchronous rotation of vibrators is employed to perform tasks like screening, crushing, and vibratory conveying of bulk materials for enhanced productivity. The synchronous mode, occurring naturally in the form of self-synchronization, was discovered and studied by I.I. Blekhman and his coworkers [1]–[3]. However, strict adherence to these conditions does not always ensure stable vibrator operation in multiple synchronization mode, underscoring the need for novel algorithmic approaches to address this challenge. For example, in [4] the features of dynamics of a vibration machine with two self-synchronizing vibration exciters of the asynchronous type are studied. The results of [4] can be used in developing resonant vibrating machine's control systems to establish the corrective values of the power supply frequency of vibration exciters in the event of an uncontrolled displacement of the technological load. The control of the resonant mode of a vibrating machine, driven by an induction motor is considered in [5], where frequency control of oscillation modes is proposed, based on measuring the phase shift between the oscillations of the working element of the VM and the exciting force. Paper [6] is devoted to the controlled vibration damping of a round plate based on a controller with phase shift adjustment in the feedback loop. The proposed controller combines the structures of regulators with positive position feedback and strain rate feedback. The experimental results are presented, where plate vibrations are measured by a laser vibrometer, and a control signal was applied to the plate using an macro fiber composites disk attached to its center. The cause of vibrational movement as an average directed motion of a material particle relative to a horizontally oscillating uniformly rough surface based on the asymmetry of the surface oscillations shape called the *temporal asymmetry*, is studied in [3], [7]–[9].

This paper focuses on developing and studying the phase shift control system of a two-rotor vibration mechatronic setup, aiming to maintain the desired revolving speed of the unbalanced rotors. Unlike [10], in the present paper, the integral component is introduced to the relay controller in the phase loop, which makes it possible to eliminate the

*This work was supported in part by the St. Petersburg State University and Russian Science Foundation project 22-11-00172. Section VI "Experimental Results" and IZ were supported by the Ministry of Science and Higher Education of the Russian Federation (project no. 124041500008-1).

[1] Department of Applied Cybernetics, Faculty of Mathematics and Mechanics, Saint-Petersburg University, Stary Peterhof, Universitetsky Prospekt, 198504 Saint Petersburg, Russia n.v.kuznetsov@spbu.ru

[2] Institute for Problems in Mechanical Engineering of Russian Academy of Sciences (IPME RAS), 61 Bol'shoy Pr. V.O., 199178 Saint Petersburg, Russia boris.andrievsky@gmail.com

[3] Khalifa University of Science and Technology, Abu Dhabi, UAE igor.boiko@ku.ac.ae

Fig. 1. Laboratory view of setup SV-2M.

static error in the phase control without the large magnitude chattering, cf. [11]. As before, PI controllers are utilized in the velocity control loops. The parameters of the Mechatronic Vibration Setup SV-2M are used for numerical study and simulations, and the experimental results are also presented.

The paper is structured as follows. Section II provides a description of the laboratory setup SV-2M, detailing its structure, technical characteristics, and presenting the adopted mathematical model of the servo system. Section III presents the proposed velocity and phase shift control laws. The possibility of sliding mode occurrence for the proposed control law is studied analytically and numerically in Section IV. Simulation results confirming the appearance of sliding mode motion and demonstrating the dynamical properties of the closed-loop system are discussed in Section V. Experimental results are described in Section VI. Finally, Section VII summarizes the obtained results and outlines future work intentions.

II. Two-Rotor Vibration Mechatronic Setup

A vibration complex SV-2M is a nonlinear electromechanical system equipped by two induction motors (IM) with unbalanced rotors. The system operates in two modes: self-synchronization of the vibrators and controlled synchronization mode [12], [13]. However, the self-synchronization mode is not always sufficiently stable due to random variations in motor and system parameters, structural oscillations. Instability in the self-synchronization mode can lead to significant deviations in the phase difference of rotor rotations from the desired values. The desired phasing of rotor rotations can also become unstable. This raises the challenge of controlling the synchronization of the electric motors, which requires measuring the rotor rotation angles and acting on the relative phase shift. The laboratory view of the setup is depicted in Fig. 1.

A. Structure and Technical Characteristics of the Laboratory Setup SV-2M

The vibration complex, considered in this work has broad research capabilities. The complex can be used to study dynamic problems such as vibration rotation, braking and starting of an unbalanced rotor, the Sommerfeld effect, self-synchronization of vibrators, synchronization control, and vibration isolation from disturbances, see [12]–[16] for more details.

B. Servo System Model

Despite the intricate dynamics of the system, our focus lies primarily on the rotation of the rotors rather than the oscillations of the platforms. Under certain conditions delineated for this study, it is justifiable to employ a simplified model that accurately captures the motor gains and principal time constants. This approach, as advocated by [13]–[16], was validated for the SV-2M system. It was determined that at low frequencies (down to 5 Hz), the gravitational (or "pendular") torque significantly influences motor rotation, necessitating consideration in controller design (cf. [17], [18]). However, at medium to high-frequency ranges (5 – 20 Hz), the phenomenon known as "averaging property" applies, wherein fast oscillating components are averaged out, and only the slower motions pertaining to revolving unbalanced rotors are pertinent, as discussed in [19], [20].

Moreover, given that induction motors incorporate local feedback controllers, the dynamics of the drive systems, including the induction motor and the frequency converter with its feedback local controller, can be approximated by the following second-order transfer function mapping the control signal to angular velocity ω:

$$W_d(s) = \left\{\frac{\omega}{u}\right\} = \frac{b_0}{a_0 s^2 + a_1 s + 1} = \frac{k_d}{T^2 s^2 + 2\xi T s + 1}, \quad (1)$$

where b_0, a_0, a_1 stand for the drive model parameters, where $b_0 = k_d$ corresponds to the drive system static gain; $T = \sqrt{a_0}$ is the time constant; $\xi = a_1 (2T)^{-1}$ denotes the damping ratio; $s \in \mathbb{C}$ stands for the Laplace transform variable. Note that the case of $\xi \geq 1$ is also possible. Model (1) is used in this work at the stage of the controller design and for the preparatory simulation.

Identification of motor model parameters was performed in [16], [21] based on the standard non-recursive least-square estimation (LSE) method, cf. [22], see details and results in [21].

III. Robust Phase-Shift Control Algorithm

Based on the approach of [21] and the speed-gradient (SG) method of [23], let us use the following control law for control of rotation speed and the phase shift between the unbalanced rotors for the two-rotor vibration setup:

$$e_{\omega_l}(t) = \omega_l^*(t) - \omega_l(t), \quad e_{\omega_r}(t) = \omega_r^*(t) - \omega_r(t), \quad (2)$$

$$\dot{\delta}_{\omega l} = e_{\omega_l}, \quad u_{\omega_l} = K_{I\omega_l}\delta_{\omega l} + K_{P\omega_l} e_{\omega_l}, \quad (3)$$

$$\dot{\delta}_{\omega r} = e_{\omega_r}, \quad u_{\omega_r} = K_{I\omega_r}\delta_{\omega r} + K_P e_{\omega_r}, \quad (4)$$

$$u_l = \mathrm{sat}_0^{u_{\max}}(u_{\omega_l} - u_\psi), \quad u_r = \mathrm{sat}_0^{u_{\max}}(u_{\omega_r} + u_\psi), \quad (5)$$

where $\mathrm{sat}_a^b(x)$ is defined as

$$\mathrm{sat}_a^b(x) = \begin{cases} a & \text{if } x \leq a, \\ b & \text{if } x \geq b, \\ x & \text{otherwice;} \end{cases}$$

the "phase-loop" control signal u_ψ is produced by the following separate algorithm, cf. [21]:

$$\psi(t) = \varphi_r(t) - \varphi_l(t), \tag{6}$$
$$e_\psi(t) = \psi(t) - \psi^*(t), \tag{7}$$
$$\Delta\omega = \omega_r - \omega_l, \tag{8}$$
$$\sigma = e_\psi + \tau_{\mathrm{M}}\Delta\omega, \tag{9}$$
$$u_\sigma = -\gamma\,\mathrm{sign}(\sigma) \tag{10}$$
$$\dot{v}(t) = u_\sigma(t), \tag{11}$$
$$u_\psi = \mathrm{sat}_{\bar{u}_\psi}\big(\tau_\sigma u_\sigma(t) + v(t)\big), \tag{12}$$

where $\mathrm{sat}_a(x) = \begin{cases} a\,\mathrm{sign}(x) & \text{if } |x| \geq a, \\ x & \text{otherwice} \end{cases}$; $\bar{u}_\psi$ is the design parameter, limiting the phase shift control signal u_ψ; τ_{M} is the "reference model" time constant; K_I and K_P are the rotation frequency controller gains; $\tau_\sigma > 0$ is the weighting factor for the phase-shift controller; $\omega^*(t)$ denotes the reference rotation frequency, while $\psi^*(t)$ stands for the reference phase shift; γ is the relay controller parameter (the relay "shelf" level). It is worth mentioning, as stated in [16], [21], [24], there are two control aims for the given vibrating setup: ensuring given rotation frequency of the unbalanced rotors as well the phase shift between there. This leads to two control contours in the setup: control of rotation frequency, which is realized by PI-controllers (2)–(4), producing control signals u_{ω_l}, u_{ω_r}, and, as in [21], the relay controller (6)–(12), generating phase control signal u_ψ. The fusion of both signals to form the control actions u_l, u_r, applied to the drives, is realized in a cross-coupling manner in (5).

Signal $\sigma(t)$, given by (9) can be treated as a first-order prediction of the phase error. In the context of systems with the sliding mode, $\sigma(t)$ corresponds to the deviation of the system's motion from the required sliding mode so that the equivalence $\sigma(t) \equiv 0$ corresponds to the specified sliding mode. From the point of view of adaptive control with an Implicit Reference Model (IRM), the algorithm represented by (6)–(12) can be referred to as the IRM algorithm, cf. [23], [25]. In the given case, the IRM is expressed by the identity $\sigma(t) \equiv 0$, and the applied control law, according to the SG method, ensures decrease of $|\sigma(t)|$. Signal σ of the form (9) can be rewritten as $\sigma = e_\psi + \tau_{\mathrm{M}}\Delta\omega = \psi^* - \psi + \tau_{\mathrm{M}}(\omega_l - \omega_r) = \psi^* - \psi - \tau_{\mathrm{M}}\dot{\psi}$. Therefore, the equivalence $\sigma(t) \equiv 0$ implies fulfillment of the relation $\tau_{\mathrm{M}}\dot{\psi} + \psi = \psi^*$, which can be called "the reference equation" by the analogy with the habitual reference model in Model Reference Adaptive Control (MRAC), as it described in [26]. Unlike the MRAC approach, the reference model

$$\tau_{\mathrm{M}}\dot{\psi}_M(t) + \psi_M(t) = \psi^*(t) \tag{13}$$

is not a part of the system but it is *implicitly* represented by parameter τ_{M} of the algorithm. This property gives the method its name. Note that the signal ψ_M is not used in the control law (2)–(5). This signal can be used to assess the reliability of the system and the achievement of the desired closed-loop behavior.

The objective is to determine the existence and time of appearance of the sliding mode (SM) in the closed-loop system (1)–(12), taking into account the presence of two control channels, each involving servo-drives described by (1) with different parameters. This topic has been extensively studied in the literature, as highlighted in references such as [23], [25], [27]. In the mentioned works, focused on the linear time-invariant (LTI) single-input–single-output (SISO) systems controlled using the relay algorithm

$$\dot{x}(t) = Ax(t) + Bu_\sigma(t), \quad \sigma(t) = GCx(t),$$
$$u_\sigma(t) = -\gamma\,\mathrm{sign}\big(\sigma(t)\big), \tag{14}$$

where $x(t) \in \mathbb{R}^n$; $u_\sigma(t) \in \mathbb{R}^1$ is defined in (10); $\sigma(t) = GCx(t) \in \mathbb{R}^1$, it was proved that a SM occurs on the surface $\sigma = 0$, if transfer function $W(s) = GC\big(s\mathbf{I} - A\big)^{-1}B \equiv \dfrac{N(s)}{D(s)}$ of (14) from control input u to measured output σ is a strictly minimal phase (SMP), i.e. if $N(s)$ is the Hurwitz polynomial, the $W(s)$ relative degree ρ, defined as $\rho = \deg D(s) - \deg N(s)$, is equal to 1, and $\gamma > 0$ is sufficiently large (with respect to a given region of initial conditions $x(0)$). Then for (14) the auxiliary control goal $\lim\limits_{t\to\infty}\sigma(t) = 0$ is achieved.

IV. Exploring Sliding Mode Potential

A. Analytical study

Firstly, let us check the SMP property for the system with control input u_ψ as in (5) and output σ, given by (9), cf. [10]. To represent the system model in the state-space LTI form $\dot{x} = Ax + Bu$, $y = Cx$ under the assumption that the saturations are not active, introduce drives state vectors $x_l = [\varphi_{\mathrm{l}}, \omega_{\mathrm{l}}, \varepsilon_{\mathrm{l}}]^{\mathrm{T}} \in \mathbb{R}^3$, $x_{\mathrm{r}} = [\varphi_{\mathrm{r}}, \omega_{\mathrm{r}}, \varepsilon_{\mathrm{r}}]^{\mathrm{T}} \in \mathbb{R}^3$, where $\varphi_{\mathrm{l,r}}$, $\omega_{\mathrm{l,r}}$, $\varepsilon_{\mathrm{l,r}}$ denote rotation angles, angular velocities, and accelerations of the left (l) and right (r) rotors respectively; variables $u_{\mathrm{l,r}}$ are taken as drive inputs u, and vectors $[\varphi_{\mathrm{l,r}}, \omega_{\mathrm{l,r}}] \in \mathbb{R}^2$ as drive outputs y. Evidentlly, the state-space representation of transfer function (1) leads to the following triples (A, B, C) in the state-space form:

$$A_{\mathrm{d,l}} = \begin{bmatrix} 0 & 1 & 0 \\ 0 & 0 & 1 \\ 0 & -1/a_{0,\mathrm{l}} & -a_{1,\mathrm{l}}/a_{0,\mathrm{l}} \end{bmatrix}, \quad B_{\mathrm{d,l}} = \begin{bmatrix} 0 \\ 0 \\ b_{0,\mathrm{l}}/a_{0,\mathrm{l}} \end{bmatrix},$$
$$A_{\mathrm{d,r}} = \begin{bmatrix} 0 & 1 & 0 \\ 0 & 0 & 1 \\ 0 & -1/a_{0,\mathrm{r}} & -a_{1,\mathrm{r}}/a_{0,\mathrm{r}} \end{bmatrix}, \quad B_{\mathrm{d,r}} = \begin{bmatrix} 0 \\ 0 \\ b_{0,\mathrm{r}}/a_{0,\mathrm{r}} \end{bmatrix},$$
$$C_{\mathrm{d}} = \begin{bmatrix} 1 & 0 & 0 \\ 0 & 1 & 0 \end{bmatrix}. \tag{15}$$

Then the transfer functions for the left and right drives from $u_{\mathrm{l,r}}$ to $y_{\mathrm{l,r}}$ are

$$W_{\mathrm{dl}}(s) = C_{\mathrm{d}}(s\mathbf{I}_2 - A_{\mathrm{dl}})^{-1}B_{\mathrm{dl}}, \quad W_{\mathrm{dr}}(s) = C_{\mathrm{d}}(s\mathbf{I}_2 - A_{\mathrm{dr}})^{-1}B_{\mathrm{dr}},$$

respectively.

Now let us take into account the PI-controllers (2)–(4) in the feedback for rotation velocities control. To this end, let us introduce the controller gain matrices (row-vectors) $G = [1, \tau_{\mathrm{M}}] \in \mathbb{R}^{1\times 2}$ and $K = [K_I, K_P] \in \mathbb{R}^{1\times 2}$ (recall that in

(3), (4) the identical controller gains for the left and right drives are taken). This leads to the following block matrices in the state-space form $\dot{x} = Ax + Bu$, $y = Cx$ for the system with input u_ψ and output σ, defined as in (6)–(9):

$$A = \begin{bmatrix} A_{\mathrm{d,l}} - B_{\mathrm{d,l}} K C_{\mathrm{d}} & \mathbf{0}_{3,3} \\ \mathbf{0}_{3,3} & A_{\mathrm{d,r}} - B_{\mathrm{d,r}} K C_{\mathrm{d}} \end{bmatrix}, \quad B = \begin{bmatrix} B_{\mathrm{d,l}} \\ -B_{\mathrm{d,r}} \end{bmatrix},$$
$$C = \begin{bmatrix} 1 & 0 & 0 & -1 & 0 & 0 \\ 0 & 1 & 0 & 0 & -1 & 0 \end{bmatrix}. \tag{16}$$

The state-space system (15), (16) representation leads to the following transfer function from input u_ψ to output σ

$$W^{\sigma}_{u_\psi}(s) = GC(s\mathbf{I}_6 - A)^{-1}B \equiv \frac{N^{\sigma}_{u_\psi}(s)}{D^{\sigma}_{u_\psi}(s)}, \tag{17}$$

where
$N^{\sigma}_{u_\psi}(s) = \tau_{\mathrm{M}}\big(a_{0,\mathrm{l}}b_{0,\mathrm{r}} + a_{0,\mathrm{r}}b_{0,\mathrm{l}}\big)s^4 + \big(a_{0,\mathrm{l}}b_{0,\mathrm{r}} + a_{0,\mathrm{r}}b_{0,\mathrm{l}} + \tau_{\mathrm{M}}(a_{1,\mathrm{l}}b_{0,\mathrm{r}} + a_{1,\mathrm{r}}b_{0,\mathrm{l}})\big)s^3$
$+\big(a_{1,\mathrm{l}}b_{0,\mathrm{r}} + a_{1,\mathrm{r}}b_{0,\mathrm{l}} + \tau_{\mathrm{M}}(b_{0,\mathrm{l}} + b_{0,\mathrm{r}} + 2b_{0,\mathrm{l}}b_{0,\mathrm{r}}K_P)\big)s^2 + (b_{0,\mathrm{l}} + b_{0,\mathrm{r}} + 2b_{0,\mathrm{l}}b_{0,\mathrm{r}}K_P + 2b_{0,\mathrm{l}}b_{0,\mathrm{r}}K_I\tau_{\mathrm{M}})s$
$+2b_{0,\mathrm{l}}b_{0,\mathrm{r}}K_I,$
$D^{\sigma}_{u_\psi}(s) = a_{0,\mathrm{l}}a_{0,\mathrm{r}}s^6 + (a_{0,\mathrm{l}}a_{1,\mathrm{r}} + a_{1,\mathrm{l}}a_{0,\mathrm{r}})s^5 + \big(a_{1,\mathrm{l}}a_{1,\mathrm{r}} + a_{0,\mathrm{l}}(b_{0,\mathrm{r}}K_P + 1) + a_{0,\mathrm{r}}(b_{0,\mathrm{l}}K_P + 1)\big)s^4$
$+ (a_{1,\mathrm{l}}(b_{0,\mathrm{r}}K_P + 1) + a_{1,\mathrm{r}}(b_{0,\mathrm{l}}K_P + 1) + a_{0,\mathrm{l}}b_{0,\mathrm{r}}K_I + a_{0,\mathrm{r}}b_{0,\mathrm{l}}K_I)s^3$
$+ ((b_{0,\mathrm{l}}K_P + 1)(b_{0,\mathrm{r}}K_P + 1) + a_{1,\mathrm{l}}b_{0,\mathrm{r}}K_I + a_{1,\mathrm{r}}b_{0,\mathrm{l}}K_I)s^2$
$+ (b_{0,\mathrm{l}}K_I(b_{0,\mathrm{r}}K_P + 1) + b_{0,\mathrm{r}}K_I(b_{0,\mathrm{l}}K_P + 1))s + b_{0,\mathrm{l}}b_{0,\mathrm{r}}K_I{}^2.$

The phase shift control law (9)–(12) introduces the integral (isodromic) factor $\dfrac{\tau_\sigma s + 1}{s}$ into the linear part, and then

$$D(s) = sD^{\sigma}_{u_\psi}(s), \quad N(s) = (\tau_\sigma s + 1)\cdot N^{\sigma}_{u_\psi}(s). \tag{18}$$

The transfer function of the system being analyzed is evidently not SMP due to its relative degree, denoted as ρ, being equal to 2. Nevertheless, certain conditions, as referenced in [28]–[31], can relax this constraint. Specifically, when $\rho = 2$, provided that γ attains a sufficiently large value, the system can achieve the auxiliary control objective of $\lim\limits_{t\to\infty}\sigma(t) = 0$.

Frequency conditions determining the presence of a SM, obtained through the Describing Functions (DF) method, are outlined in [28], [30]. In [28], the correlation between the relative degree of a plant's transfer function and the likelihood of SM occurrence in relay systems is examined using the Locus of a Perturbed Relay System (LPRS) approach, introduced in [32]. The LPRS, defined as a characteristic of the response of a linear component to unequally spaced pulse control of variable frequency in a closed-loop, serves as the basis for understanding SM behavior.

Drawing on the LPRS concept, it is demonstrated in [28], [32] that if $\rho = 1$ or 2 and the LPRS exhibits no intersection points with the real axis apart from the origin, the ideal SM manifests. In such instances, the frequency of chattering tends toward infinity, resulting in an infinite equivalent gain. This assertion is formalized in the following Theorem.

Theorem 1: ([30, Theorem 4.5]). If the transfer function $W(s)$ is a quotient of two polynomials $N(s)$ and $D(s)$ of degrees m and n, respectively, with non-negative coefficients, then for the existence of ideal SM, it is necessary that the relative degree $\rho = n - m$ of $W(s)$ be one or two. If $\rho = 1$, then a conventional ideal SM can appear; if $\rho = 2$, then the so-called asymptotic second-order SM can occur, see [33], [34].

As stated in [30], Theorem 1 does not provide a sufficient condition, as a periodic motion of a finite frequency can exist even if the relative degree is one or two [28]. In [28] an example is demonstrated showing that if the LPRS intersects the real axis from below, returns then to the lower half-plane, and finally approaches the origin of the coordinates from below having the real axis as an asymptote, the SM appears in some vicinity of the stationary state. In this case, the SM appears only if initial conditions are sufficiently small.

B. Numerical study

Let us analyze the system properties numerically for the specific values of the system model parameters, taken from [21]:

- Left drive parameters: $b_{0,\mathrm{l}} = 0.0042$ s^{-1}, $a_{0,\mathrm{l}} = 0.1187$ s^2, $a_{1,\mathrm{l}} = 0.8110$ s.
- Right drive parameters: $b_{0,\mathrm{r}} = 0.0043$ s^{-1}, $a_{0,\mathrm{r}} = 0.1185$ s^2, $a_{1,\mathrm{r}} = 1.2195$ s.
- Reference model time constant: $\tau_{\mathrm{M}} = 2$ s.
- The following values of rotation frequency controller (2)–(5) gains K_I, K_P were set equal for both the right and left drives as $K_I = 240$, $K_P = 1680$ s.
- The desired rotation frequency is set to the constant value $\omega^* = 40$ rad/s for both drives,
- The natural bounds of control signals saturation are [0 – 40000], therefore $u_{\max} = 40000$ in (5).

However, fulfillment of the frequency condition ensures the existence of a sliding mode; τ_σ should be sufficiently large. Then the LTI closed-loop system dynamics with the given in (18) polynomials are described by the following equation

$$\big(D(p) + \gamma N(p)\big)\sigma(t) = 0, \tag{19}$$

where $p = \mathrm{d}/\mathrm{d}t$ denotes the time derivation operator.

The roots locus and the Nyquist plots for the cases of $\tau_\sigma = 0.01$ s and $\tau_\sigma = 5$ s are depicted in Figs. 2, 3, respectively.

V. Simulation Results

To confirm the conclusion made, let us simulate the complete system, including the plant model (18), tracking the reference action by the drives' angular velocities, and the relay law of phase shift control. The control law is given by (2)–(12), $\gamma = 2500$, $\tau_{\mathrm{M}} = 2$ s, $\tau_\sigma = 2$ s, $\omega^* = 40$ rad/s, $\psi^* = \pi$.

As is seen from time histories of $\sigma(t)$, $u_\psi(t)$, $\psi(t)$, $\omega_{\mathrm{l}}(t)$, $\omega_{\mathrm{r}}(t)$, depicted in Fig. 4, the controlled variables $\psi(t)$, $\omega_{\mathrm{l}}(t)$, $\omega_{\mathrm{r}}(t)$ tend to the desirable (reference) values ψ^*, ω^*, and the sliding mode occurs asymptotically, cf. [33], [34].

It is worth emphasizing that the simulations were performed solely to illustrate the analytical results for an idealized model, that exactly corresponds to equations (2)–(12), (18) and without considering the real factors impacting the system's behavior. In particular, for the chattering

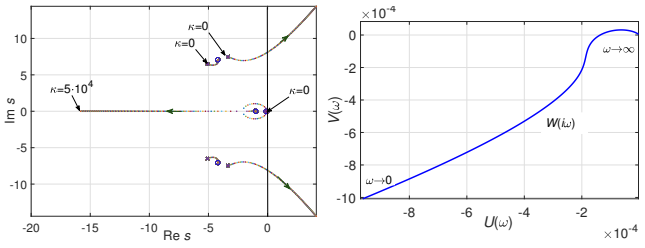

Fig. 2. Root locus (left plot), Nyquist chart (right plot); $\tau_\sigma = 0.01$ s.

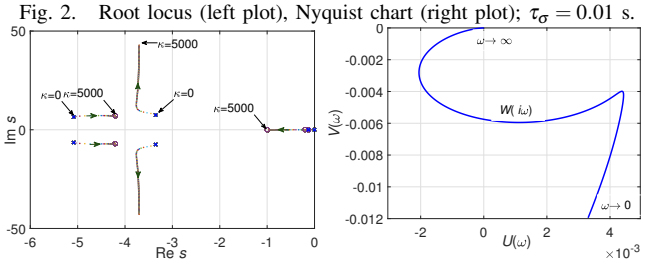

Fig. 3. Root locus (left plot), Nyquist chart (right plot); $\tau_\sigma = 5$ s.

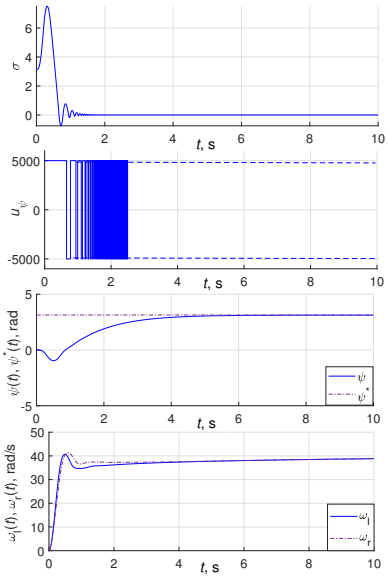

Fig. 4. Simulation results. Time histories of $\sigma(t)$, $u_\psi(t)$ (upper plot) and $\psi(t)$, $\omega_l(t)$, $\omega_r(t)$ (lower plot).

phenomenon not to be noticeable, the Euler method of the *MATLAB/Simulink* package with the sufficiently small step of 10^{-3} s was used in the simulation.

In reality, the following factors affect the system's behavior:

1. The angular velocities ω_l, ω_r are calculated based on sampled measurements of the quantized rotation angles φ_l, φ_r with sampling time T0=0.01 s, quantization step $2\pi/4000$ rad, and consequent discrete-time differentiating.

2. The induction drive dynamics models contain, apart from the induction motors dynamics' complexity, the *Schneider Electric* frequency converter *Altivar ATV12H018M2* with its local feedback law, not revealed by the manufacturer. The dry friction effect, existing in the drives, can also be hardly estimated.

3. The rotors revolving is strongly affected by the vibrations of the stand, which has essentially nonlinear dynamics, that hardly be taken into account due to its complexity and

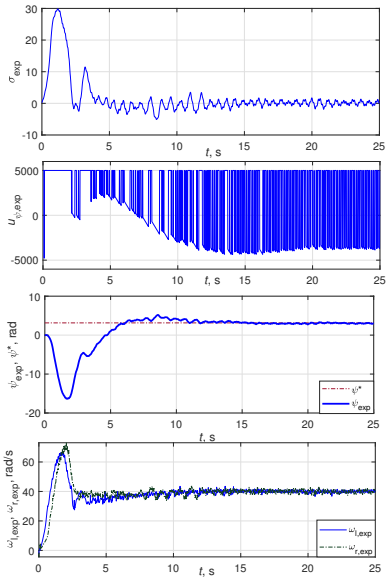

Fig. 5. Experimental results. Time histories of $\sigma_{\text{exp}}(t)$, $u_{\psi,\text{exp}}(t)$ (upper plot) and $\psi_{\text{exp}}(t)$, $\omega_{\text{l,exp}}(t)$, $\omega_{\text{r,exp}}(t)$ (lower plot).

numerous unknown parameters, cf. [16].

All these features can not be adequately reproduced by simulations, but experimentally only. A number of the experimental results are presented in the previous works, see [13], [15], [16], [21], [24], [35], [36]. Some specific experimental results related to control law (2)–(12) are given below in Sec. VI.

VI. Experimental Results

All the experiments have been carried out on the mechatronic vibrational setup MMLS SV-2M, as described in Section II. The desired rotation frequency $\omega^* = 40$ rad/s was set to both rotors. The PI-controller gains for rotational frequency were taken as $k_I = 240$, $k_P = 1680$ s, both for right and left motor loops. Control law (2)–(12) parameters were taken as $\gamma = 2500$, $\tau_{\text{M}} = 2$ s, $\tau_\sigma = 2$ s. The controller sampling interval T_s was 0.01 s. The IRM (13) time constant $\tau_M = 1$ s was taken. In (12), $\bar{u}_\psi = 5000$ was set.

The experimental results, obtained for the same conditions as the simulation ones, are plotted in Fig. 5. These results, in general, fit the simulation ones, but, naturally, the chattering manifests itself, and it is evident that in reality, the transients are not as fast as in the idealized system model.

VII. Conclusion

This paper presents the successful development and examination of a phase shift control system tailored for a two-rotor vibration mechatronic setup, with the objective of sustaining the desired revolving speed of the unbalanced rotors. The implementation of sliding mode motion was accomplished by integrating a relay controller into the phase loop, while PI controllers were deployed in the velocity control loops. By conducting numerical investigations and simulations utilizing the parameters of the Mechatronic Vibration Setup SV-2M from IPME RAS, the effectiveness of the proposed velocity and phase shift control strategies was validated.

Analytical and numerical studies were conducted to explore the potential occurrence of sliding mode behavior within the phase shift loop, confirming its asymptotical existence. Simulations illustrated this mode's appearance and elucidated the closed-loop system's dynamic properties.

In summary, the outcomes of this investigation affirm the efficiency of the phase shift control system in attaining the desired rotor speed and underscore the feasibility of introducing sliding mode motion into the mechatronic setup. Future endeavors aim to refine and optimize the control system based on the acquired insights and investigate additional applications and enhancements for the two-rotor vibration mechatronic setup. Additionally, the inclusion of the "square-root" multiplier in the control law, inspired by the super-twisting method proposed by [37], [38], as discussed in [21], warrants further exploration in subsequent studies.

ACKNOWLEDGMENTS

The Authors are grateful to V.I. Boikov for his invaluable work in creating the electronic and computer facilities of the MMLS SV-2M.

REFERENCES

[1] I. I. Blekhman and N. P. Yaroshevich, "Multiple modes of vibratory maintenance of rotation of unbalanced rotors," *Proceedings of the Academy of Sciences of the USSR. Machine Science*, pp. 62–67, 1986, (in Russian).

[2] I. I. Blekhman, *Vibrational Mechanics*. Moscow: Phys.-math. lit., 1994, (in Russian).

[3] I. I. Blekhman, V. B. Vasil'kov, and Y. A. Semenov, "Vibrotransporting of bodies on a surface with non-translational rotational oscillations," *J. Machinery Manufacture and Reliability*, vol. 49, no. 4, pp. 280–286, 2020.

[4] A. Gouskov, G. Panovko, and A. Shokhin, "To the issue of control resonant oscillations of a vibrating machine with two self-synchronizing inertial exciters," *Lecture Notes in Mechanical Engineering*, vol. 58, pp. 515–526, 2021.

[5] G. Panovko, A. Shokhin, and S. Eremeikin, "The control of the resonant mode of a vibrating machine that is driven by an asynchronous electro motor," *J. Machinery Manufacture and Reliability*, vol. 44, no. 2, pp. 109–113, 2015.

[6] L. Leniowska and M. Sierże, "Vibration control of a circular plate using parametric controller with phase shift adjustment," *Mechatronics*, vol. 58, pp. 39–46, 2019.

[7] I. I. Blekhman and G. Y. Dzhanelidze, *Vibrational Movement [Vibratsionnoye peremeshcheniye]*. M.: Nauka, 1964, (in Russian.

[8] I. Lyan and G. Panovko, "Modelling the granular medium dynamics on rough vibrating plane using method of large particles," *IOP Conf. Series: Materials Science and Engineering*, vol. 489, no. 1, 2019.

[9] A. M. Vasiliev, S. A. Bredikhin, and V. K. Andreev, "On the issue of vibration displacement with non-harmonic oscillations of the working surface [k voprosu o vibratsionnom peremeshchenii pri negarmonicheskikh kolebaniyakh rabochey poverkhnosti]," *Scientific journal NRU ITMO. Ser. Processes and Food Production Equipment*, no. 2, pp. 42–48, 2019, in Russian.

[10] N. Kuznetsov, B. Andrievsky, I. Zaitceva, and E. Akimova, "Sliding-mode control of phase shift for two-rotor vibration setup," *Lecture Notes in Computer Science (including subseries Lecture Notes in Artificial Intelligence and Lecture Notes in Bioinformatics)*, vol. 14214 LNAI, pp. 221–232, 2023.

[11] P. Kaveh, A. Ashrafi, and Y. Shtessel, "Integral and second order sliding mode control of harmonic oscillator," in *Proceedings of the 44th IEEE Conference on Decision and Control*, 2005, pp. 3941–3946.

[12] B. R. Andrievskii, I. I. Blekhman, L. I. Blekhman, V. I. Boikov, V. B. Vasil'kov, and A. L. Fradkov, "Education and research mechatronic complex for studying vibration devices and processes," *J. Mach. Manuf. Reliab.*, vol. 45, no. 4, pp. 369–374, 2016.

[13] V. I. Boikov, B. Andrievsky, and V. V. Shiegin, "Experimental study of unbalanced rotors synchronization of the mechatronic vibration setup," *Cybernetics and Physics*, vol. 5, no. 1, pp. 5–11, 2016.

[14] B. Andrievsky, V. I. Boikov, A. L. Fradkov, and R. E. Seifullaev, "Mechatronic laboratory setup for study of controlled nonlinear vibrations," *IFAC-PapersOnLine*, vol. 49, no. 14, pp. 1–6, 2016, 6th IFAC Workshop on Periodic Control Systems PSYCO 2016.

[15] B. Andrievsky, A. L. Fradkov, O. P. Tomchina, and V. I. Boikov, "Angular velocity and phase shift control of mechatronic vibrational setup," *IFAC-PapersOnLine*, vol. 52, no. 15, pp. 436–441, 2019.

[16] A. L. Fradkov, O. P. Tomchina, B. Andrievsky, and V. I. Boikov, "Control of phase shift in two-rotor vibration units," *IEEE Trans. Control Syst. Technol.*, vol. 29, no. 3, pp. 1316–1323, 2021.

[17] D. A. Tomchin and A. L. Fradkov, "Control of passage through a resonance area during the start of a two-rotor vibration machine," *J. Machinery Manufacture and Reliability*, vol. 36, no. 4, pp. 380–385, 2007.

[18] A. Fradkov, O. Tomchina, and D. Tomchin, "Controlled passage through resonance in mechanical systems," *J. Sound and Vibration*, vol. 330, no. 6, pp. 1065–1073, 14 March 2011.

[19] I. I. Blekhman, *Vibrational Mechanics: Nonlinear Dynamic Effects, General Approach, Applications*. Singapore: World Scientific, 2000.

[20] ——, *Synchronization in Nature and Technology: Theory and Applications*. New York: ASME Press, 1988.

[21] B. Andrievsky, I. Zaitceva, and I. Barkana, "Passification-based robust phase-shift control for two-rotor vibration machine," *Electronics*, vol. 12, no. 4, 2023.

[22] L. Ljung, *System Identification: Theory for the User*. Upper Saddle River, NJ, USA: Prentice Hall, Jan. 1999.

[23] A. L. Fradkov, I. V. Miroshnik, and V. Nikiforov, *Nonlinear and Adaptive Control of Complex Systems*. Dordrecht: Kluwer, 1999.

[24] B. Andrievsky and V. I. Boikov, "Bidirectional controlled multiple synchronization of unbalanced rotors and its experimental evaluation," *Cybernetics And Physics*, vol. 10, no. 2, pp. 63–74, 2021.

[25] B. R. Andrievskii and A. Fradkov, "Method of passification in adaptive control, estimation, and synchronization," *Autom. Remote Control*, vol. 67, no. 11, pp. 1699–1731, 2006.

[26] J. D. Landau, *Adaptive control systems. The model reference approach*. New York, NY: Dekker, 1979.

[27] B. Andrievsky and A. Fradkov, "Implicit model reference adaptive controller based on feedback Kalman–Yakubovich lemma," in *IEEE Conference on Control Applications (CCA'94)*, vol. 2, 1994, pp. 1171–1174.

[28] I. Boiko, "Analysis of modes of oscillations in a relay feedback system," in *2004 American Control Conference*, vol. 2, 2004, pp. 1253–1258 vol.2.

[29] A. Fradkov, "Passification of linear systems with respect to given output," in *2008 47th IEEE Conference on Decision and Control*, 2008, pp. 646–651.

[30] I. Boiko, *Discontinuous Control Systems. Frequency-Domain Analysis and Design*. Boston: Birkhäuser, 2009.

[31] I. M. Boiko, N. V. Kuznetsov, R. N. Mokaev, and E. D. Akimova, "On asymmetric periodic solutions in relay feedback systems," *Journal of the Franklin Institute*, vol. 358, no. 1, pp. 363–383, 2021.

[32] I. Boiko, "Input-output analysis of limit cycling relay feedback control systems," in *1999 American Control Conference (Cat. No. 99CH36251)*, vol. 1, 1999, pp. 542–546 vol.1.

[33] ——, "On phase deficit of the super-twisting second-order sliding mode control algorithm," *International Journal of Robust and Nonlinear Control*, vol. 30, no. 16, pp. 6351–6362, 2020.

[34] I. M. Boiko, "On frequency-domain criterion of finite-time convergence of second-order sliding mode control algorithms," *Automatica*, vol. 47, no. 9, pp. 1969–1973, 2011.

[35] B. Andrievsky and I. Zaitceva, "Symmetrical control law for chaotization of platform vibrations," *Symmetry*, vol. 14, no. 11, 2022. [Online]. Available: https://www.mdpi.com/2073-8994/14/11/2460

[36] I. Zaitceva, B. Andrievsky, and L. Sivachenko, "Enhancing functionality of two-rotor vibration machine by automatic control," *Cybernetics and Physics*, vol. 12, no. 4, pp. 289–295, 2023.

[37] A. Levant, "Sliding order and sliding accuracy in sliding mode control," *Int. J. Control*, vol. 58, no. 6, pp. 1247–1263, 1993.

[38] G. Bartolini, A. Levant, A. Pisano, and E. Usai, "Adaptive second-order sliding mode control with uncertainty compensation," *Intern. J. Control*, vol. 89, no. 9, pp. 1747–1758, 2016.